

# A 60 Joule, 600KV, 1ns Rise-time Marx System

M.M. Kekez, J. LoVetri, A.S. Podgorski, J.G. Dunn, G. Gibson

Division of Electrical Engineering,  
National Research Council, Ottawa, Canada,  
K1A 0R8

## ABSTRACT

This paper describes work on the design and development of a low-energy Marx generator system capable of producing a fast (1 ns rise-time)  $\pm 600$  kV pulse. The system consists of a Marx generator, peaking circuit and a short length coaxial line with a passive load. The generator delivers the power to 10-150 ohm loads with a peak power approaching 10 GW. The unique features are simplicity of design, ease of operation, and above all compactness which permits easy portability and in-situ application. The system can be used: a) to produce an intense relativistic electron/ion beam in the virtual-cathode reflex triode for high power microwave generation; b) for flash X-ray radiography to record and study dynamic events where interposed material, debris, or flame exclude the use of high speed cameras; c) to provide  $10^6$  to  $10^7$  D-D (2.45 MeV) or D-T (14.1 MeV) neutrons in several nanoseconds; d) to study the dielectric properties of matter; e) for NEMP studies; and f) to preionize a powerful (electron beam controlled) eximer laser system. Experimental results are presented along with computer simulations using lumped-parameter approximations.

## 1. INTRODUCTION

Four decades ago Fletcher [1] constructed an impulse generator system capable of delivering 20-50 kV impulses with a rise-time of 0.4 ns into a high (83.3 ohm) impedance load. As a result of the development of the micro-oscillograph, the capacitive (E-dot probe) divider, and the pulse-sharpening switch, he studied the formative time lag of spark breakdown in the 0.4-100 ns range as a function of applied electric field strength across a gap. His work has enabled the study of ionization processes on shorter time scales.

Consequently, a number of papers followed reporting on such studies. Specifically, the effect of intensity and duration of UV irradiation on the formative time lag was investigated in great detail by the Russian school (ie. Academician G.A. Mesyats et. al. [2]) in the late 60's. They observed that with intense irradiation of the cathode, the statistical component of formative time lag is eliminated and that the rate of current rise (during the transition from insulating gas to a highly conducting arc) is a strong function of UV radiation, effecting several orders of magnitude change in formative time lag characteristics.

New understanding in optically controlled discharges came as a result of the use of lasers to initiate the spark breakdown. The ever increasing diversity of wavelengths available today, coupled with advances in high time resolution diagnostic techniques are allowing a deeper understanding of the processes involved in switching technology, as well as demonstrating precise timing and synchronization capabilities to well below 1 picosecond. Recent advances in optically controlled discharges (>10 MV and peak powers of  $10^{12}$  -  $10^{14}$  W with nominal voltage rise times of < 10 ns delivered to transducers) are reviewed by Guenther and Bettis [3].

In spite of current improvements in laser reliability and efficiency of interaction of the optical coupling (particularly in resonant mode) of the laser beam to the gas in the switch, we have, in part due to economic considerations, resorted to UV controlled discharges. This was achieved by arranging that each stage of the Marx bank provide a hard UV source which photoionizes each consequent stage of the bank, hence insuring a spatially uniform avalanche development in the channel plasma. It has been experimentally established that: a) the dominant ionizing radiation

occurs at wavelengths below 1000 angstroms; and that b) the effective photon mean free path for photoionization is up to 10 cm in some gas mixtures designed by gas engineering techniques for pulsed power and switching.

After adopting Fletcher's operating point for each stage, an appropriate gas should be found which meets the following criteria: the passage of large current; high voltage hold-off; and transport of UV radiation to provide a volumetric photoelectron density in excess of  $10^9/\text{cm}^3$  at the next stage of the Marx bank. (The "gas dielectric engineering" is actively studied in Prof. G. Christophorou's group in Knoxville [4]).

## 2. FORMULATION

Design goals were formulated at the beginning of this project. These are shown in Table 1.

Table 1

Marx Generator Specifications	
Parameter	Value
maximum available output peak voltage	960 KV
nominally operational output peak voltage	600 KV
minimum operational output peak voltage	100 KV
rise time (10% to 90%)	< 1ns
decay time (1/e definition)	12-90 ns
repetitive pulse generation at 600 KV level	1 ppm
trigger jitter	< 10 nsec
trigger voltage	10 V
prepulse	< 5%
repeatability	< 10%
load	10 - 150 ohm
polarity	dual

In order to achieve these goals, the following design decisions were made:

a) The generator is designed in the form of a coaxial structure. Thus the capacitors, connecting leads, and spark gaps, together with the enclosure, lead to the establishment of a fast forming line.

b) Optically controlled erection of the Marx is governed by UV irradiation. Advances in gas engineering for pulsed power is employed to ensure minimum jitter in closing time of individual switches enabling a semi-constant value of through-put time for the system. In addition, the gas must have a sufficiently high standoff voltage to avoid excessive pressurization of the vessel (< 3 atmospheres).

c) To minimize the weight of the system and to avoid an oil filled enclosure for the d.c. power supply, each stage of the Marx is charged up to 40 kV, whereas the nominal operational point is 25-28 kV. This corresponds to Fletcher's condition for each stage.

d) In accordance with H.V. engineering practices, each energy storage stage is guarded by a *corona ring* and the joining leads are terminated by *hemi-spheres*. Also H.V. charging resistors are imbedded in an elastomer to protect them from debris.

### 3. DESIGN

#### 3.1 Preliminary Experimentation

A prototype 8 stage plus sharpening switch, 200 kV Marx was initially built to examine the design concepts. In some ways this prototype resembles that of Platts [5]. An experimental study of the timing sequence of the spark breakdown for the 9 switches was made. A typical *streak camera* recording of the closing sequence is shown in figure 1. Graphical results for three gas combinations (SF<sub>6</sub>, N<sub>2</sub> and 10% SF<sub>6</sub> - 90% Ar) are shown in figure 2. Surprisingly, a relatively low jitter has been observed for all three gas combinations. A similar study for the 24 stage Marx will be attempted in the future.

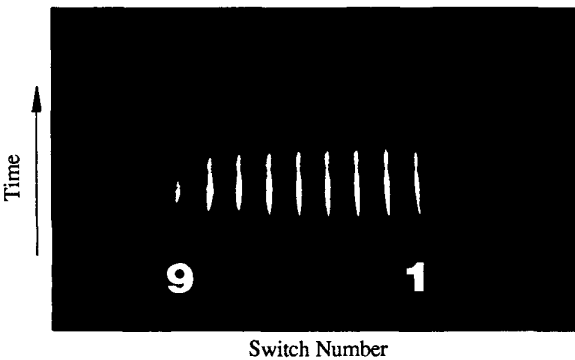


Fig. 1: Typical Streak Recording

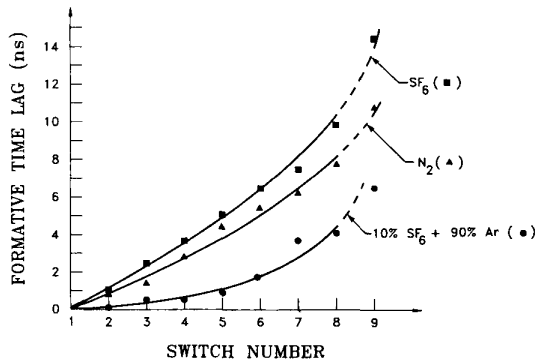


Fig. 2: Timing Sequence for 3 Gas Mixtures

#### 3.2 Computational Circuit Analysis

A simple computer model based on the experimental Marx switch closure times was developed. Three stages of the Marx as well as the peaking capacitor circuit were implemented in the computer model. Each stage was approximated by:

a) an 8.1 nF series charging capacitance;

b) a 4 pF capacitance from the center of the coaxial structure to the outside shell;

c) a 15 nH series inductance to take into account the inductance of the leads as well as the inductance of the closed switch channel;

d) and a time delayed switch.

The peaking capacitor circuit was approximated by a 5 nH lead/switch inductance and a 35 pF charging parallel capacitance. This was the value of the peaking capacitor which was used in the 600 kV Marx. The load was modelled by an 8 nH inductance in series with a 100 ohm, 4pF parallel combination to ground. Details of this model are shown in figure 3.

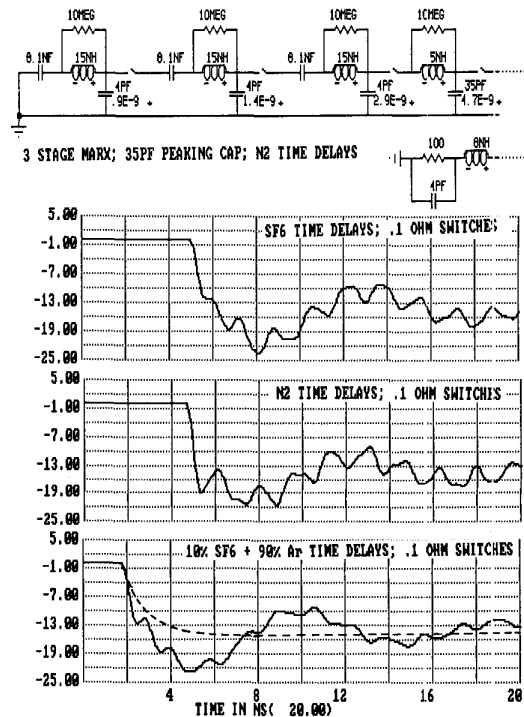


Fig. 3: Computer Simulation of Circuit Model

A time domain analysis was performed on this circuit model with the switch time delays as shown in Table 2. These were derived from the experimental results performed on the 9 stage Marx. Results of the calculated output voltage (across the 100 ohm load) for each of the time delays, representative of the three gases used, are also shown in figure 3. The last switch closure time was increased in order to properly simulate the peaking capacitor circuit which cannot be obtained from figure 2. This circuit was independently pressurized in the 600 kV Marx (i.e. independent control of closure time). Considering the crudeness of the circuit model, the waveform results are remarkably informative. The figures show the great dependence of the output waveforms on the sequential timing of the switches. The waveforms also demonstrate a qualitative similarity to the experimentally measured waveforms discussed below. The last trace of figure 3 contains (broken line superimposed on the actual waveform) the theoretical waveform for a double exponential pulse having time constants of 1 ns and 270 ns (determined from the RC time constant of the circuit model).

Table 2

Experimental Switch Time Delays			
Switch No.	Time Delay (ns)		
	SF6	N <sub>2</sub>	10%SF6; 90% Ar
T1	1.0	0.9	0.1
T2	2.5	1.4	0.5
T3	3.75	2.9	0.55
T4	5.0	4.7	1.8

### 3.3 Final design of 600kV Marx

A cross-sectional view of the 600 kV Marx is shown in figure 4. The spark gaps consist of 1 inch brass spheres placed 2.8 mm apart. Each stage uses 2.7 nF, 40 kV Murata capacitors. These are joined by the plate inside the corona guard rings which are extended to form a connection by 10-32 screws to the spark gap electrodes. The rail is supported by 9-inch diameter plexiglass tubing of .5 inch wall thickness. Figure 5 shows the assembly of the 24 stages prior to being placed into the plexiglass shell (figure 6). The 12 inch diameter aluminum cylinder provides the enclosure for the vessel as well as the current return path. The stress analysis of the assembly suggested that the weakest point is at the output of the Marx which consists of a 3 inch thick plexiglass flange attached via *acrofix* glue. A stress breaking point capability of 5.5 atmospheres was estimated.

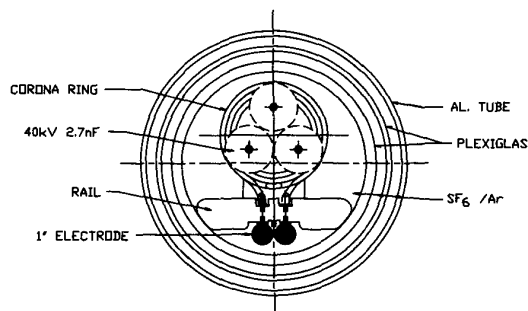


Fig. 4: Cross-sectional View of 600 kV Marx

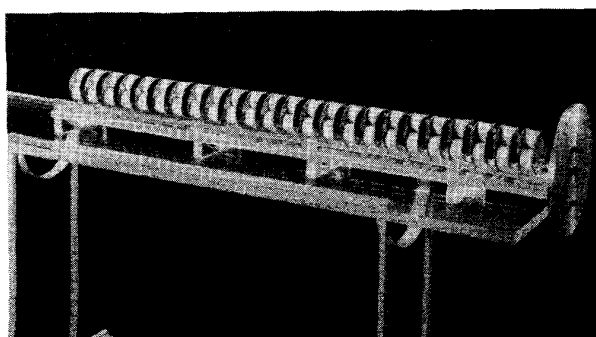


Fig. 5: 24 Stage Assembly

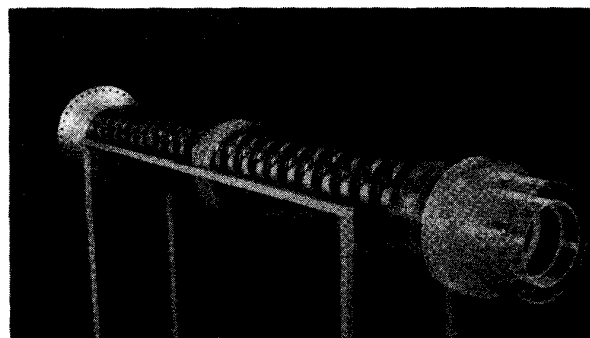


Fig. 6: Assembly in the Shell

To achieve reliable operation the spark gap is subjected to approximately 70 % of the self breakdown voltage. This reduces the risk of pre-fire during operation.

Following the earlier work on the self-similar properties of minimum sparkover voltages in air of a rod-plane (0.1-30m) gap (in both polarities) by Kekez [6], the experimental evidence has been summarized for SF<sub>6</sub>, transformer oil, mylar, PPM and PE. The curves of the sparkover voltage vs gap distance can be described in terms of: a) the minimum amount of energy per unit length supplied to the developing spark channel to enable the channel to elongate; and b) the corresponding average value of the electric field, which supplies the energy to the channel. In this work (to be published), the finding by Cooke and Cookson [7] are supported. That is, the main parameters governing the value of the breakdown field (in small gaps) are the mass density of dielectrics and the time duration of the applied voltage. In a zero order approximation, it is immaterial whether the matter is in gaseous, liquid and/or solid form.

A practical solution is to use a heavy electronegative gas such as SF<sub>6</sub>. As stated in the introduction the effective photo mean free path in the gas should be sufficiently long to photo-preionize volumetrically the subsequent stage in the Marx bank. Mixtures of two or more gases (with additives) offer an opportunity to achieve better high voltage insulating performance than obtainable with the individual gases. (In the case of N<sub>2</sub> and SF<sub>6</sub>, 20 % SF<sub>6</sub> by pressure raises the breakdown strength to about 80 % that of pure SF<sub>6</sub>). At the same time such mixtures should allow maximum UV transport and photoionization due to modifications in discharge processes, kinetics and energy distribution.

An individually pressurized peaking capacitor circuit is used. This allows independent control of the final switch closure time which the computer models have shown has a great effect on the pulse waveform. A capacitance value of 35 pF was obtained using an oil filled chamber. This value equals about 10% of the erected capacity of the Marx generator.

## 4. DESIGN VERIFICATION

The generator was tested for a coaxial load configuration. The load consisted of a 1.5 m long 100 ohm coaxial line terminated with a coaxial water resistor. The value of the water resistor was varied from a few ohms to 100 ohms.

The generator impulse waveform was measured with the use of an E-field sensor installed on the outer shell of the load's coaxial line. The sensor was installed 6 inches from the peaking capacitor circuit. The sensor used to perform the measurements was an NRC developed wideband (300 kHz to 3 GHz) capacitive E-field device. A low loss 50 ohm 10.4 m long coaxial cable was used to connect the E-field sensor to a TEK 7250 digitizer having a 6 GHz bandwidth.

For load resistances higher than 50 ohms, the output pulse recorded was of double exponential shape. The duration of the pulse is governed by the value of the load impedance and does not affect

the measured rise-time. Frequency domain data was obtained from the sampled waveforms via the use of an FFT algorithm. The purpose of this is to try to extract time domain characteristics (such as pulse rise-time) from the frequency domain data by comparing to theoretical frequency domain data for double exponential waveforms. For double exponential waveforms the *knee-frequency* at which the 20 dB/decade roll-off changes to a 40 dB/decade roll-off can be related to the 10-90% rise time by (see Lee [8]):

$$T_r = 1.1/\pi f \quad ; \quad \text{for double-exponential wave-form;}$$

$$T_r^* = 2.2/\pi f \quad ; \quad \text{for inverse double-exponential wave-form;}$$

However for a 100 ohm water resistor required to terminate the 100 ohm coaxial line, the comparison was not possible. The experimental knee-frequency was in the order of several GHz corresponding to a rise-time of well under 0.1 ns. This did not compare with the time-domain measured rise-time. A possible explanation for this is that the pulse sharpening switch assumes the role of virtual-cathode reflex triode used for high power microwave generation. There, electrons reflexing in the potential well between the virtual and the real cathode, oscillate in space and time causing the microwave emission during the pulse. As in the work by

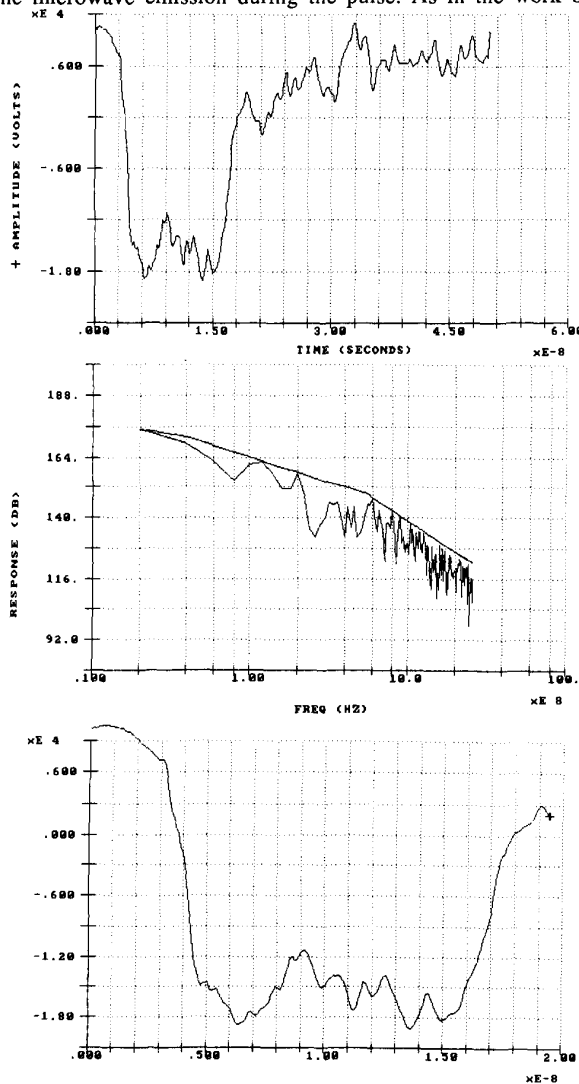


Fig. 7: Time Domain and FFT Results in N<sub>2</sub>

Burkhart et. al. [9], specifically dedicated to achieving a maximum conversion efficiency from the pulsed power to the microwave power, our frequency spectrum also shows several peaks in the GHz range.

In order to avoid the microwave emission and excitation of frequency components in the 3 GHz range, (the resonant frequency of the E-field sensor) the pulse length was reduced to 12 ns by reducing the load resistance to its lowest possible value. The generated impulse lost its double exponential character. However, the rise time measurements were not effected. The results are shown in figures 7 and 8. The trace (top) refers to the data after the probe transfer function is taken into account. To determine the rise-time the waveform was expanded (bottom). The resulting rise-time and knee-frequencies derived from figures 7 and 8 are 1.08 ns, 0.98 ns, and 580 MHz and 600 MHz respectively. A 580 MHz knee-frequency corresponds to a  $T_r = 0.604$  ns and  $T_r^* = 1.207$  ns while the 600 MHz knee-frequency corresponds to a  $T_r = 0.58$  ns and  $T_r^* = 1.16$  ns. Our time domain results thus correspond well to both the double exponential waveforms with closer correlation to the more realistic inverse double exponential waveform.

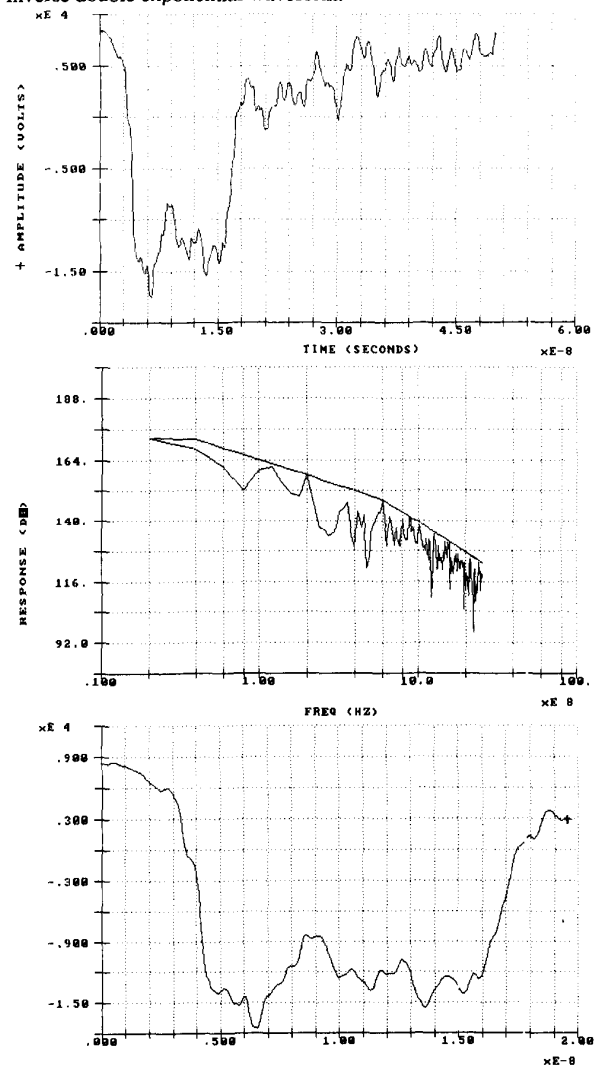


Fig. 8: Time Domain and FFT Results in 10% SF<sub>6</sub> + 90% Ar

## 5. CONCLUSIONS

Preliminary experimental data have been presented which meet the goals stated in Table 1. In addition to *tuning* the system by choosing the most appropriate gas composition, further pulse sharpening will be attempted via magnetic insulation techniques. In the ingenuous work by DiCapua et. al. [10] and Adler [11] this technique was used to achieve a five-fold improvement (15 to 3 ns) in results. Our aim is to apply similar techniques in the sub-nanosecond range.

## ACKNOWLEDGEMENTS

The authors are indebted to Dr. M.M.C. Collins and Mr. S.A. Mayman for their interest in the project. Special thanks are due to Messrs: C.C. Eamer, A.R. Taylor, B.C. Farr, N.W. Preece and A. Macadam for their part in the development of the system. Thoughts were translated into drawings by Mr. R. Vallieres. Figure 2 was obtained by Mr. S. Sychaleun.

## REFERENCES

- [1] R.C. Fletcher, "Impulse breakdown in 10<sup>-9</sup>-sec. range of air at atmospheric pressure", Phys. Rev., Vol. 76, No. 10, pp. 1501-1511, Nov. 15, 1949, also "Production and measurement of ultra-high speed impulses", Rev. Sci. Inst., Vol. 20, No. 12, pp. 861-869, Dec. 1949.
- [2] G.A. Mesyats, Yu I. Bychkov and V.V. Kremnev, "Pulsed nanosecond discharges in gases", Sov. Phys. Uspekhi, Vol. 15, pp. 282-297, 1972.
- [3] A.H. Guenther and J.R. Bettis, "Recent advances in optically controlled discharges" (invited paper), IEE Conf. Gas Discharges and their Applications, Venice, Italy, 1988, to be published also "The laser triggering of high-voltage switches", J. Phys. D: Appl. Phys., Vol. 11, pp. 1577-1613, 1978.
- [4] L.G. Christophorou, D.L. McCorkle and S.R. Hunter, "Gas mixtures for spark closing switches with emphasis on efficiency of operation", 5th Gas Dielectric Conf., 1987, pp. 381-388.
- [5] D. Platts, "10-Joule 200 kV mini marx", 5th IEEE Pulse Power Conference, Arlington, Virginia, U.S.A., June 10-12, pp 834-836, 1985.
- [6] M.M. Kekez, "Self-similar properties of minimum spark over voltage in air for both polarities in rod-plane (0.1-30m) gaps", J. Phys. D: Appl. Phys., Vol. 18, pp. 1813-1823, 1985.
- [7] C.M. Cooke and A.H. Cookson, "The nature and practices of gases as electric insulators", IEEE Electr. Insul., Vol. EI-13, No. 4, pp. 239-248, Aug. 1978.
- [8] K.S.H. Lee (ed.), EMP Interaction Principles, Techniques and Reference Data, Hemisphere Publ. Corp., Washington, 1986.
- [9] S.S. Burkhart, R.D. Scarpetti and R.L. Lundberg, "A virtual-cathode reflex triode for high-power microwave generation", J. Appl. Phys., Vol. 58, No. 1, pp. 28-36, 1 July 1985.
- [10] M.S. DiCapua, D.A. Goerz, K. Freytag, "Vacuum Transmission Lines for Pulse Sharpening and Diagnostic Applications", 6th IEEE Pulsed Power Conference, Arlington, Virginia, U.S.A., June 10-12, pp 393-396, 1987.
- [11] R.J. Adler, "Fast rise-time pulsed power technology", U.S. Patent, 1987, Also: "Fast rise-time pulsed power experiment", AMRC-R-737, MRC, Albuquerque, NM, 1986.